ATLAS results on open heavy quark production

Leonid Gladilin
(Moscow State University)

On behalf of the ATLAS Collaboration

LHC physics day on "Charm and bottom quark production at the LHC"

CERN, December 3rd 2010

Outline :

$D^{*\pm}$, $D^{\pm}$ and $D_s^{\pm}$ reconstruction (ATLAS-CONF-2010-034)

$B^{\pm} \rightarrow J/\psi\, K^{\pm} \rightarrow (\mu^+\mu^-)\, K^{\pm}$ reconstruction (ATLAS-CONF-2010-097)

$e^{\pm}$ from HQ decays (ATLAS-CONF-2010-073)

$\mu^{\pm}$ from HQ decays (ATLAS-CONF-2010-075)

HQ jets (ATLAS-CONF-2010-099)

$D^{(*)}$-mesons reconstruction

For *D*-meson reconstruction: 1.4 nb^{-1}
(March-May, minimum-bias trigger after prescale)

No *dE/dx* particle identification (not effective for high-p_T tracks)

Selection Strategy:

To select D-mesons one can utilise:

- hard nature of charm production $(p_T(D^{(*)}),\ p_T(K,\pi))$
- hard nature of charm fragmentation $(p_T(D^{(*)})/E_T)$
- relatively large D-mesons' life-times (l_{XY})
- "spin" angular behaviours of D-mesons' decays $(\cos\theta^*,\ \cos\theta')$

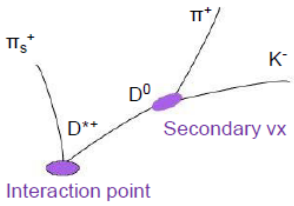

Goals:

- use widest kinematic range where signals can be measured

  $p_T(D^{(*)}) > 3.5\,\mathrm{GeV},\ \ |\eta(D^{(*)})| < 2.1$
- make signals as clean (significant) as possible in the kinematic range
- use cuts (their values) which do not produce large systematic uncertainties

To tune actual cut values realistic MC has been used

PYTHIA with ATLAS Geant4 simulation (arXiv:1005.4568)

$D^{*+} \to D^0\pi^+ \to (K^-\pi^+)\pi^+$ (+c.c.) reconstruction

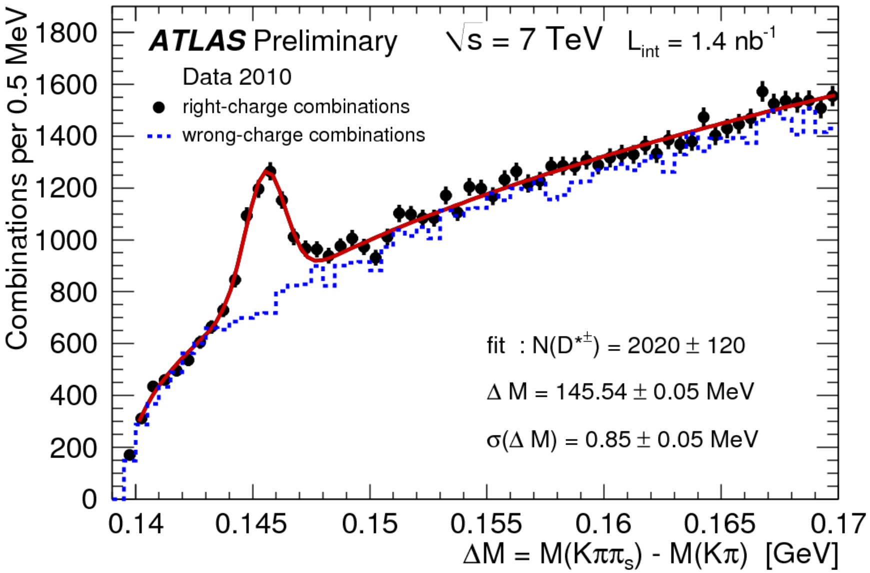

Kinematic range:

$p_T(D^{*\pm}) > 3.5\,\mathrm{GeV},\ |\eta(D^{*\pm})| < 2.1$

$p_T(D^{*\pm})/\sum E_T > 0.02 \quad \Leftarrow$ **hard fragmentation**

$L_{XY}(D^0) > 0 \quad \Leftarrow c\tau(D^0) = 123\,\mu\mathrm{m}$

$p_T(K,\pi) > 1\,\mathrm{GeV},\ p_T(\pi_s) > 0.25\,\mathrm{GeV}$

$\Leftarrow 1.83 < M(K\pi) < 1.90\,\mathrm{GeV}$

Wrong-charge combinations: $(K^+\pi^+)\pi_s^-$ (+ c.c.)

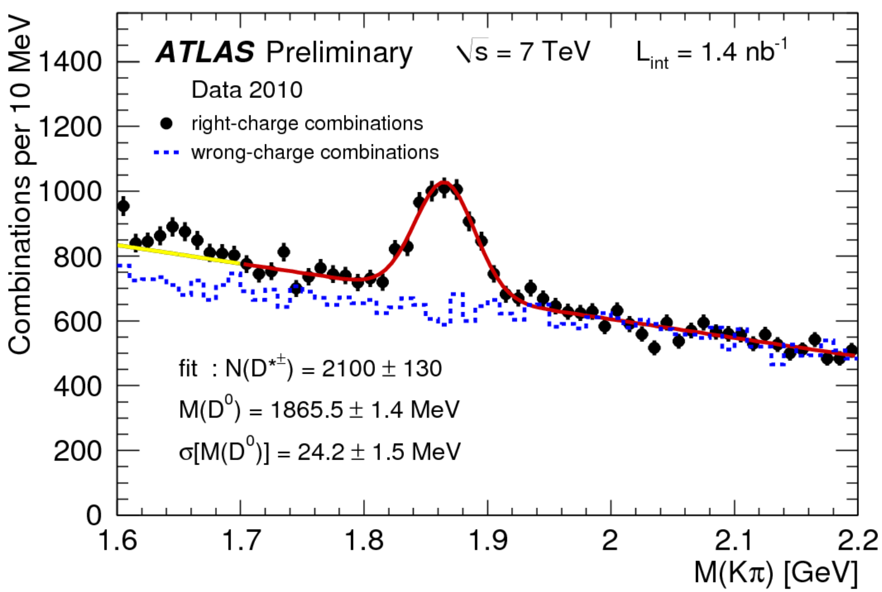

$\Leftarrow 144 < M(K\pi\pi) - M(K\pi) < 147\,\mathrm{MeV}$

Fitted masses and widths consistent with MC and PDG mass values

$D^+ \to K^- \pi^+ \pi^+$ (+c.c.) reconstruction

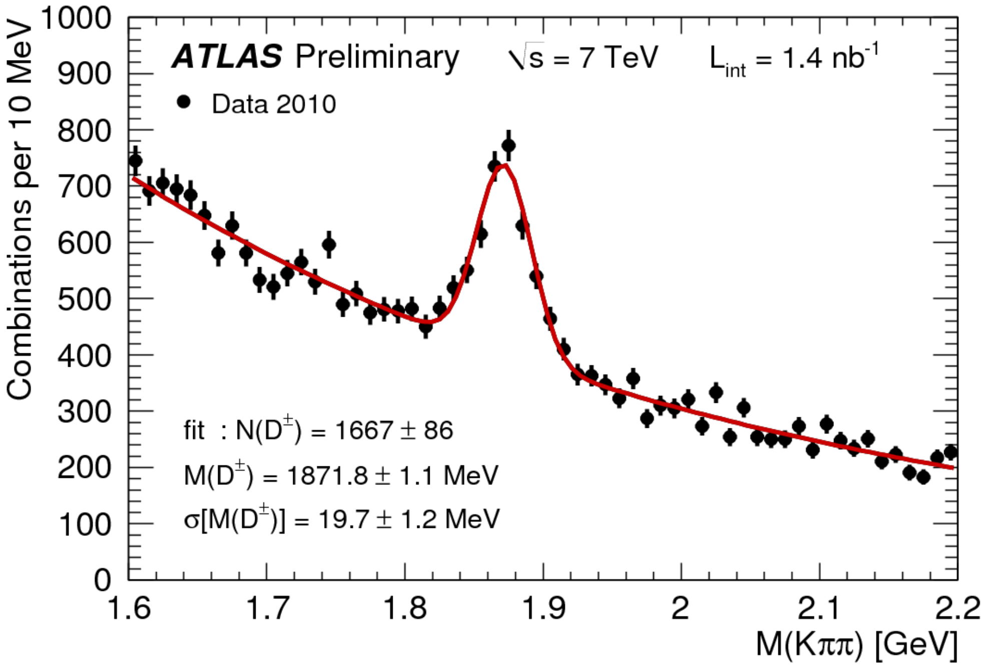

Kinematic range:

$p_T(D^\pm) > 3.5\,\mathrm{GeV},\ |\eta(D^\pm)| < 2.1$

$p_T(D^\pm)/\sum E_T > 0.02$ $\Leftarrow$ **hard fragmentation**

$L_{XY}(D^\pm) > 1.3\,\mathrm{mm}$ $\Leftarrow$ $c\tau(D^+) = 312\,\mu\mathrm{m}$

$p_T(K) > 1\,\mathrm{GeV}$

$p_T(\pi_{1,2}) > 0.8\,\mathrm{GeV},\ p_T(\pi_{1,2}^{\max}) > 1\,\mathrm{GeV}$

suppression of $D^{*\pm}$ and $D_s^+ \to \phi\,\pi^+ \to (K^-\,K^+)\,\pi^+$ (+c.c.) reflections:

remove $\Delta M_{1,2} < 150\,\mathrm{MeV}$ and $|M(K^\pm, "K^\mp") - M(\phi)_{\mathrm{PDG}}| < 8\,\mathrm{MeV}$

$\cos\theta^*(K) > -0.8$ (angle between $\vec{p}(K)$ in $D^\pm$ rest frame and $\vec{p}(D^\pm)$ in the lab)

Fitted mass and width consistent
with MC and PDG mass value

$D_s^+ \to \phi\pi^+ \to (K^-K^+)\pi^+$ (+c.c.) reconstruction

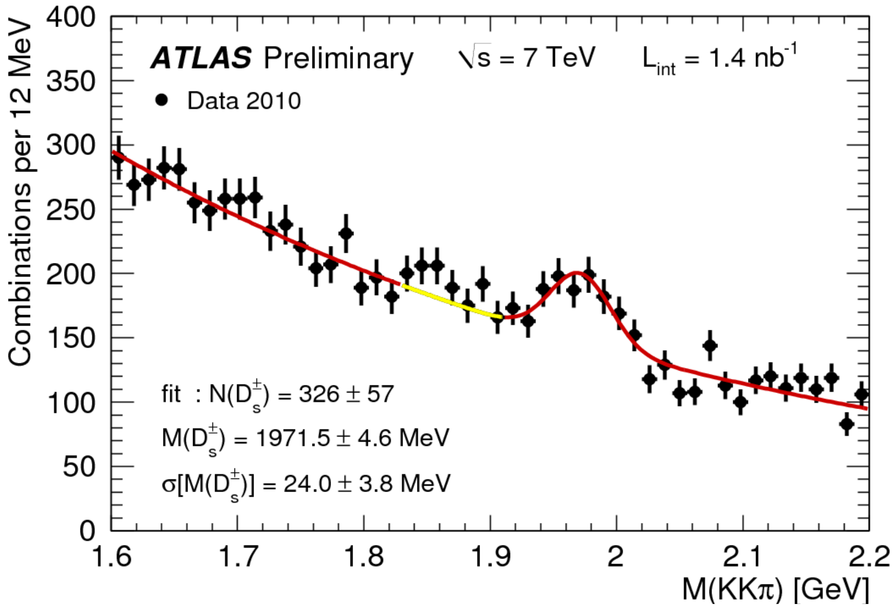

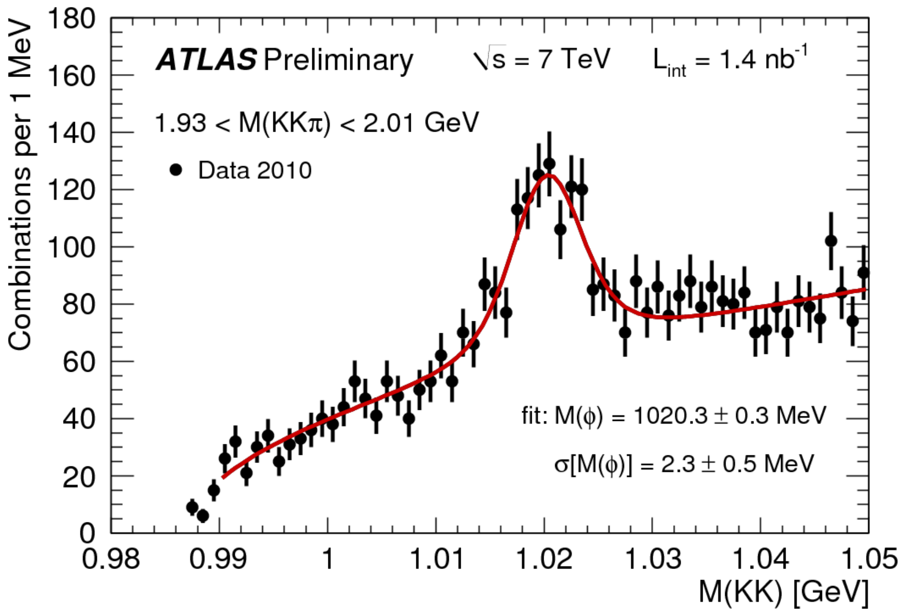

Kinematic range:

$p_T(D_s^\pm) > 3.5\,\mathrm{GeV},\ |\eta(D_s^\pm)| < 2.1$

$p_T(D_s^\pm)/\sum E_T > 0.04$ $\Longleftarrow$ **hard fragmentation**

$L_{XY}(D_s^\pm) > 0.4\,\mathrm{mm}$ $\Longleftarrow c\tau(D_s^+) = 150\,\mu\mathrm{m}$

$p_T(K_{1,2}) > 0.7\,\mathrm{GeV},\ p_T(\pi) > 0.8\,\mathrm{GeV}$

$\Longleftarrow |M(KK) - M(\phi)_{\mathrm{PDG}}| < 6\,\mathrm{MeV}$

$\cos\theta^*(\pi) < 0.4$
($\angle$ between $\vec{p}(\pi)$ in $D_s^\pm$ r.f. and $\vec{p}(D_s^\pm)$ in the lab)

$|\cos\theta'(K)|^3 > 0.2$
($\angle$ between $\vec{p}(K)$ and $\vec{p}(\pi)$ in K^+K^- r.f.)

$\Longleftarrow 1.83 < M(KK\pi) < 1.91\,\mathrm{GeV}$

Fitted masses and widths consistent with MC and PDG mass values

NLO predictions to confront with cross sections expected soon

Used : MC@NLO, POWHEG-HERWIG, POWHEG-PYTHIA (NLO+PS MC, public codes)

To be involved : FONLL (NLO+NLL), GM-VFNS (variable flavour number)
Expected : MC@NLO+PYTHIA, NNLO ?

Is it the same "NLO" in all predictions ?

$\sqrt{s} = 14\,\mathrm{TeV}$, CTEQ6m, $m_b = 4.75\,\mathrm{GeV}$, $m_c = 1.5\,\mathrm{GeV}$

MC@NLO 3.41:

$$\mu^2 = m_Q^2 + \frac{(p_{T,Q} + p_{T,\bar{Q}})^2}{4}$$

$$\sigma_{b\bar{b}} = 0.457 \pm 0.001\,\mathrm{mb} \quad \sigma_{c\bar{c}} = 6.539 \pm 0.020\,\mathrm{mb}$$

POWHEG-hvq 1.01:

$$\mu^2 = m_Q^2 + (M_{Q\bar{Q}}^2/4 - m_Q^2) \cdot \sin^2(\theta_Q)$$

$$\sigma_{b\bar{b}} = 0.464 \pm 0.001\,\mathrm{mb} \quad \sigma_{c\bar{c}} = 5.312 \pm 0.010\,\mathrm{mb}$$

Comment from Stefano Frixione:

MC@NLO returns a total cross section identical to that computed by the underlying NLO computation. This is not the case for Powheg; extra terms, beyond NLO, are included. These are NOT, however, the result of a proper NNLO computation (or beyond). Thus, large differences between MC@NLO and Powheg reflect our ignorance on the predictions beyond NLO.

Hadronisation and theoretical uncertainties

Hadronisation : HERWIG cluster model or Bowler modification of Lund symmetric fragmentation function

Fragmentation fractions set to LEP data :

	LEP data	
	stat.⊕syst.	br.
$f(c \to D^{*+})$	0.235 ±0.007	±0.003
$f(c \to D^{+})$	0.222 ±0.010	±0.009
$f(c \to D_s^{+})$	0.087 ±0.009	±0.005
$f(b \to D^{*\pm})$	0.175 ±0.020	±0.001
$f(b \to D^{\pm})$	0.227 ±0.016	±0.010
$f(b \to D_s^{\pm})$	0.140 ±0.016	±0.008

Theoretical uncertainties :

- scale uncertainty. The uncertainty was determined by varying μ_r and μ_f independently to $\mu/2$ and 2μ, with the additional constraint $1/2 < \mu_r/\mu_f < 2$, and selecting the largest positive and negative variations;
- m_Q uncertainty. The uncertainty was determined by varying the charm and bottom quark masses independently by 0.2 GeV and 0.25 GeV, respectively. The total m_Q uncertainty was obtained by adding the positive and negative cross-section variations in quadrature;
- PDF uncertainty. The uncertainty was determined by using the CTEQ6.6 PDF error eigenvectors. The total PDF uncertainty was obtained by adding the positive and negative cross-section variations in quadrature;
- hadronisation uncertainty. This uncertainty was obtained for each $D^{(*)}$ meson as a sum in quadrature of the corresponding fragmentation fraction uncertainty and the fragmentation function uncertainty. The latter uncertainty was determined in frame of the POWHEG-PYTHIA predictions by using the Peterson fragmentation function [26] with extreme choices of the fragmentation parameter: 0.02 and 0.1 for charm fragmentation, and 0.002 and 0.01 for beauty fragmentation. The uncertainties of the fragmentation fractions originating from the uncertainties in the charm meson decay branching ratios were not included into the total hadronisation uncertainties because they affect experimental and theoretical cross-section calculations in the same way and can be ignored in the comparison.

$B^{\pm} \rightarrow J/\psi\, K^{\pm} \rightarrow (\mu^{+}\mu^{-})\, K^{\pm}$ reconstruction

A variety of single and di-muon triggers, $L_{int} = 3.4\ pb^{-1}$

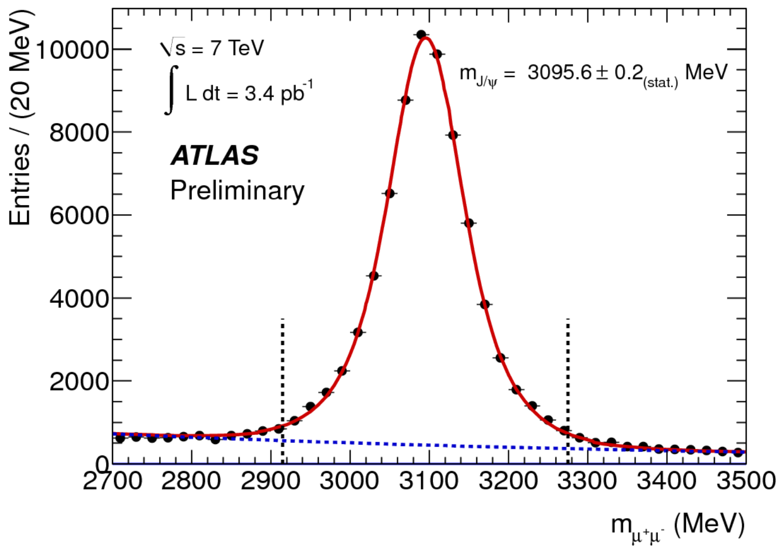

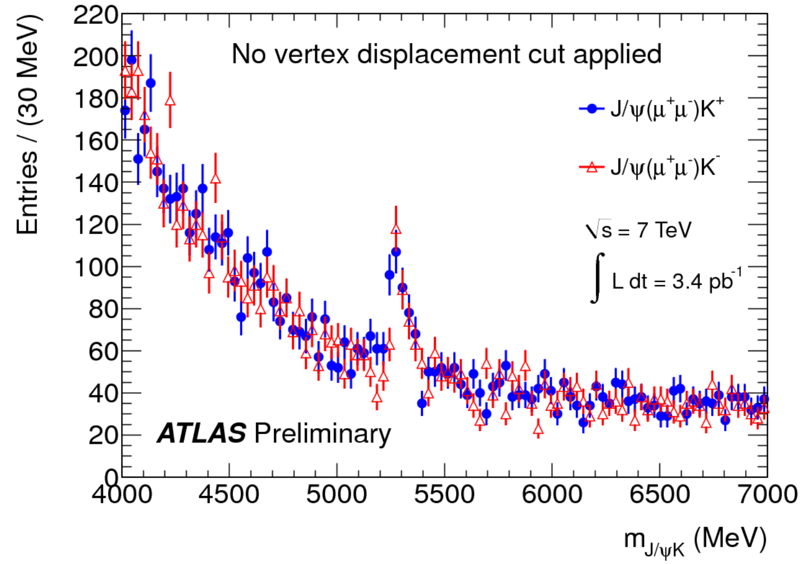

$p_T(\mu_1) > 4$ GeV, $p_T(\mu_2) > 2.5$ GeV, $|\eta(\mu)| < 2.5$

a common vertex ($\chi^2 < 10$)

$2915 < M(\mu^+\mu^-) < 3275$ MeV ($\pm 3\ \sigma$)
kept for $B^{\pm}$ reconstruction

an additional track (no PID) with
$p_T > 2.5$ GeV, $|\eta| < 2.5$

a common 3-track vertex ($\chi^2 < 6$)
with $M(\mu^+\mu^-)$ constrained to $M(J/\psi)_{PDG}$

$p_T(B^{\pm}) > 10$ GeV

$B^{\pm} \rightarrow J/\psi\, K^{\pm} \rightarrow (\mu^{+}\mu^{-})\, K^{\pm}$ signals

No cut on transverse decay length (L_{XY})

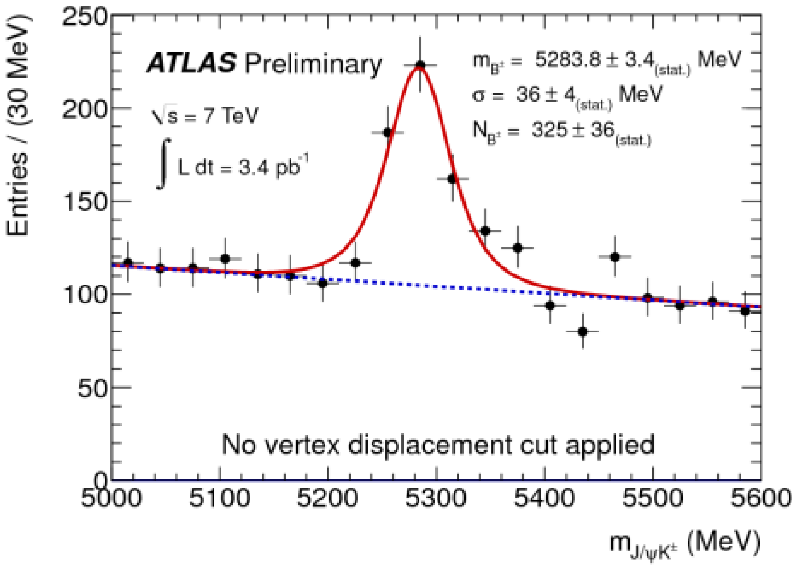

$L_{XY} > 300$ μm

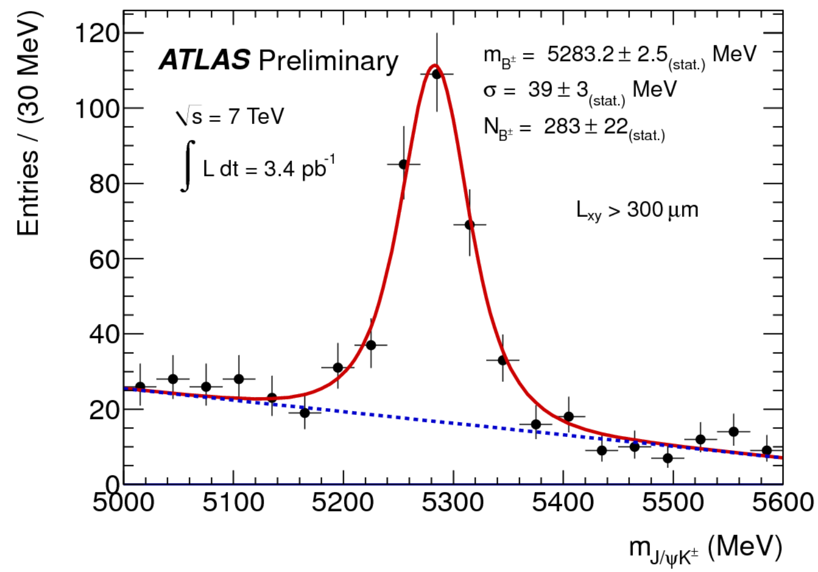

unbinned likelihood fit:

$$L = \prod_{i=1}^{N} F_{signal}(m^{i}_{J/\psi K}) + F_{bkg}(m^{i}_{J/\psi K})$$

$$F_{signal}(m_{J/\psi K}) \equiv f_{sig} \frac{1}{\sqrt{2\pi}\, S\, \delta m_{J/\psi K}} e^{\frac{-(m_{J/\psi K} - m_{B\pm})^2}{2(S\,\delta m_{J/\psi K})^2}}$$

$$F_{bkg}(m_{J/\psi K}) \equiv \frac{1 - f_{sig}}{m_{max} - m_{min}} \left[1 + b\left(m_{J/\psi K} - m_C\right)\right]$$

$$m_C \equiv (m_{max} + m_{min})/2$$

Fitted mass and width consistent with MC and PDG mass value

$e^{\pm}$ from HQ decays

Level 1 EM (3 GeV) calorimeter trigger, $L_{int} = 13.8\ nb^{-1}$

electron reconstruction: cluster in EM calorimeter matched to a track

$E_T > 7$ GeV (high trigger efficiency)

$|\eta| < 2.0$ (transition radiation tracker, TRT, coverage)

except $1.37 < |\eta| < 1.52$ (crack between barrel and end-cap EM cal.)

Still a mixture of hadrons, $e^{\pm}$ from photon conversions, and prompt $e^{\pm}$ ($Q \rightarrow e$)

To separate 3 components use 2 variables:

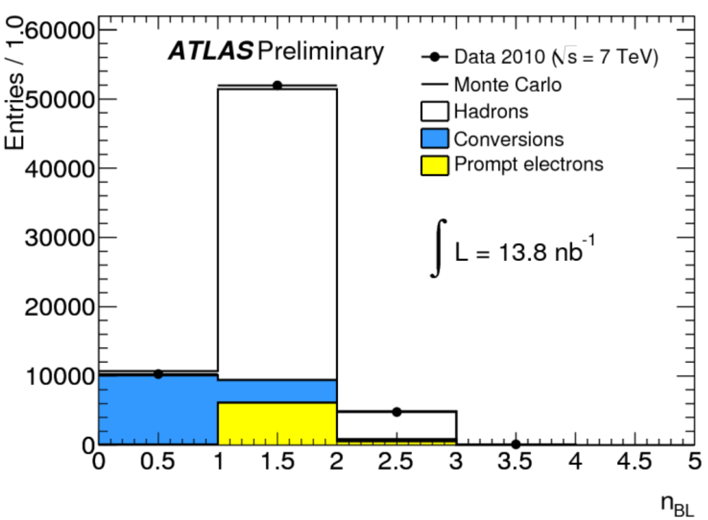

hits in innermost layer (B-layer, R = 50 mm)

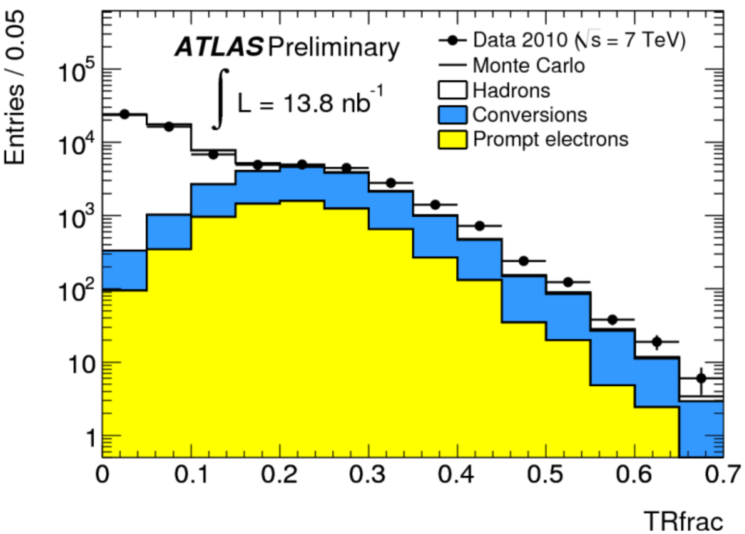

Fraction of high-threshold TRT hits

Components were separated using matrix of their measured and simulated efficiencies vs n_{BL} and TRfrac

Distributions of $e^{\pm}$ from HQ decays

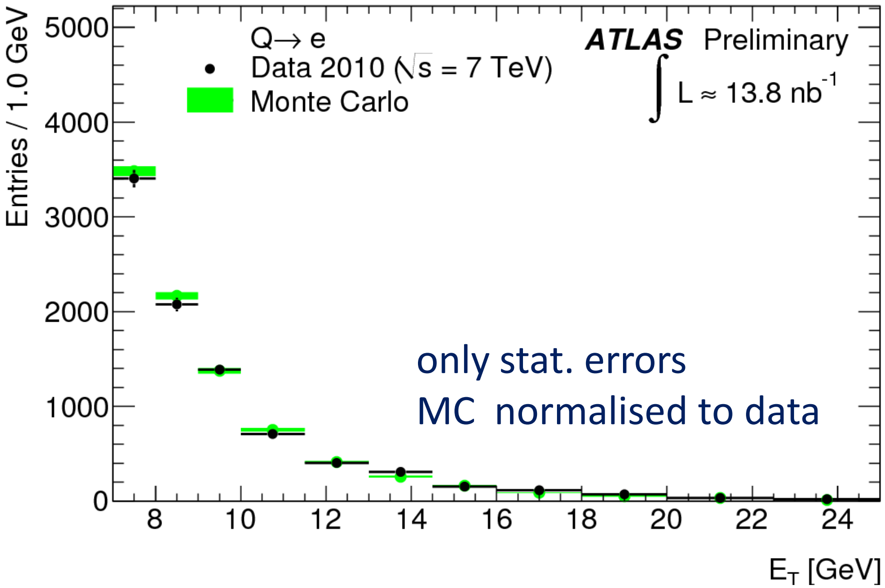

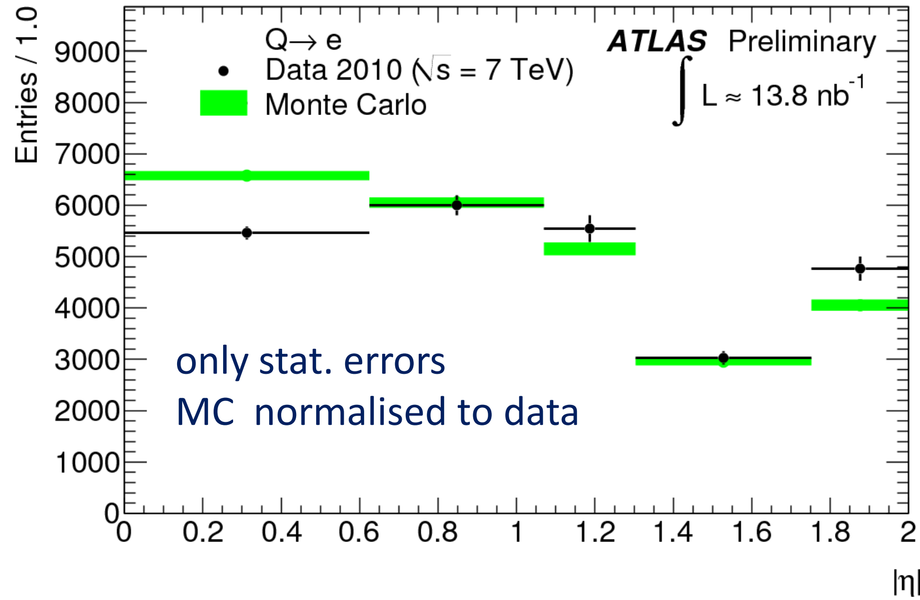

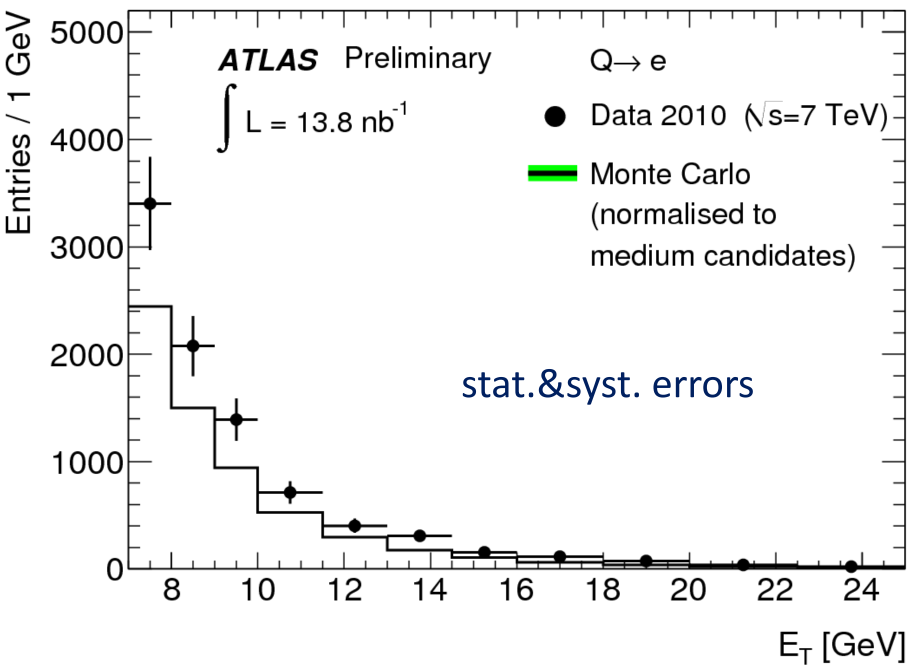

$N(Q \rightarrow e) = 9920 \pm 160\,(\text{stat.}) \pm 990\,(\text{syst.})$

systematic uncertainties are dominantly due to the extraction procedure variations

reasonable agreement with MC in shapes

← HQ fraction underestimated by the MC ?

differential cross sections soon

$\mu^{\pm}$ from HQ decays

softest muon trigger w/o threshold, L_{int} = 17 nb^{-1}

muon reconstruction: match of a track in the inner detector (ID) with a track in the muon spectrometer (MS), common fit

$p_T > 4$ GeV, $|\eta| < 2.5$

to separate from π and K decays use →

where p_{param} – energy loss parametrisation

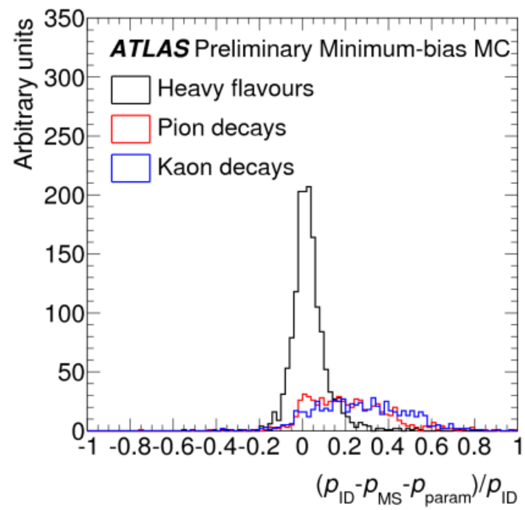

templates for HQ, π and K decays were simulated and verified with data

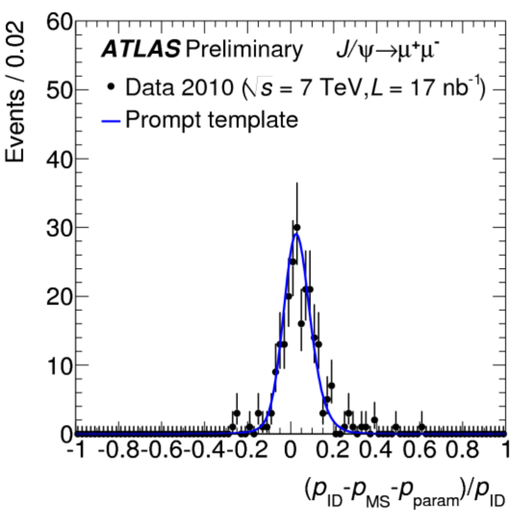

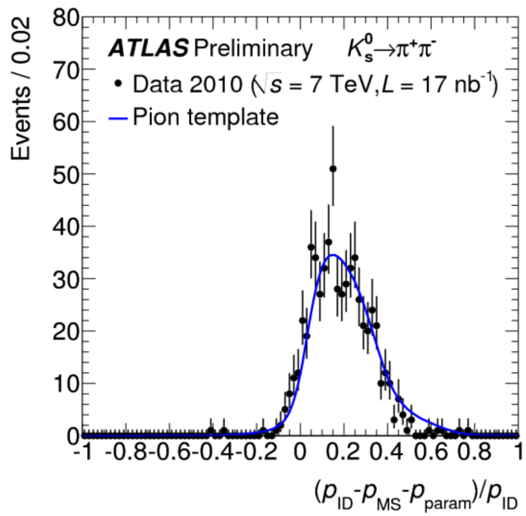

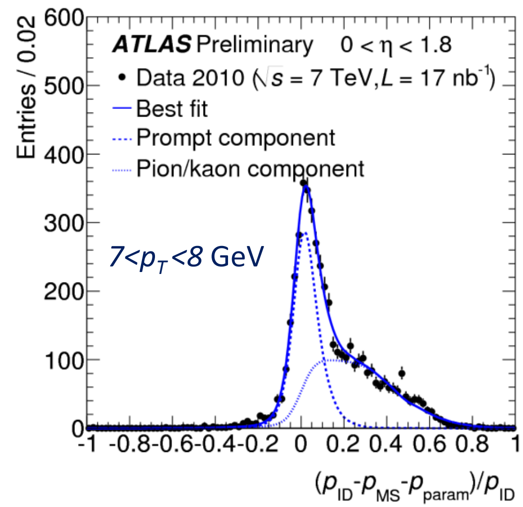

fit performed in each bin

Fractions of μ$^{\pm}$ from HQ decays

N(μ$^{\pm}$ *) = 157466* in full sample, fractions of prompt muons measured

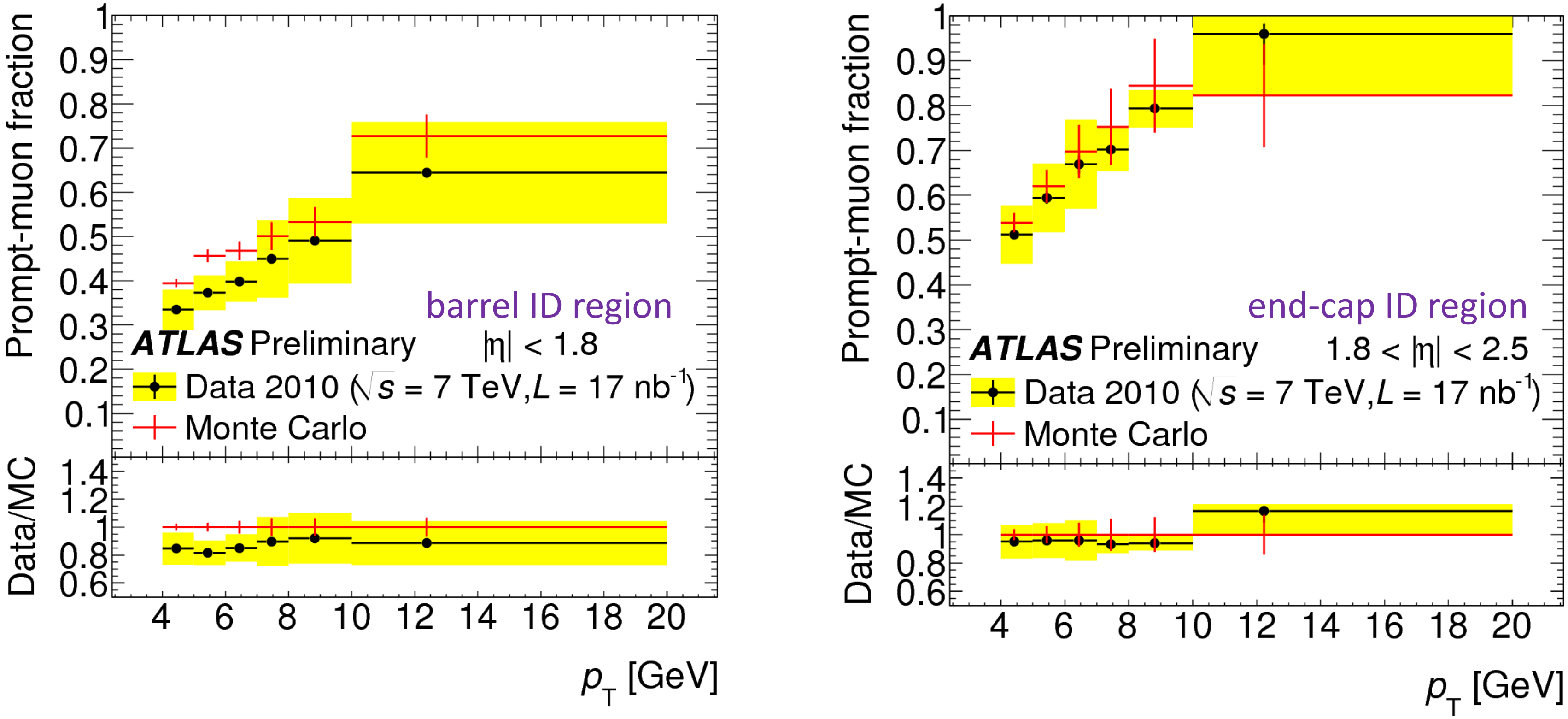

bands – are sums in quadrature of the fit and systematic uncertainties on templates

prompt *μ*$^{\pm}$ fraction increases rapidly with p_T*(μ*$^{\pm}$ *)*

minimum-bias MC describes data fractions

HQ Jets

many studies on various b-tagging aspects

can be used for b-jet cross-section measurements

soft lepton tagging

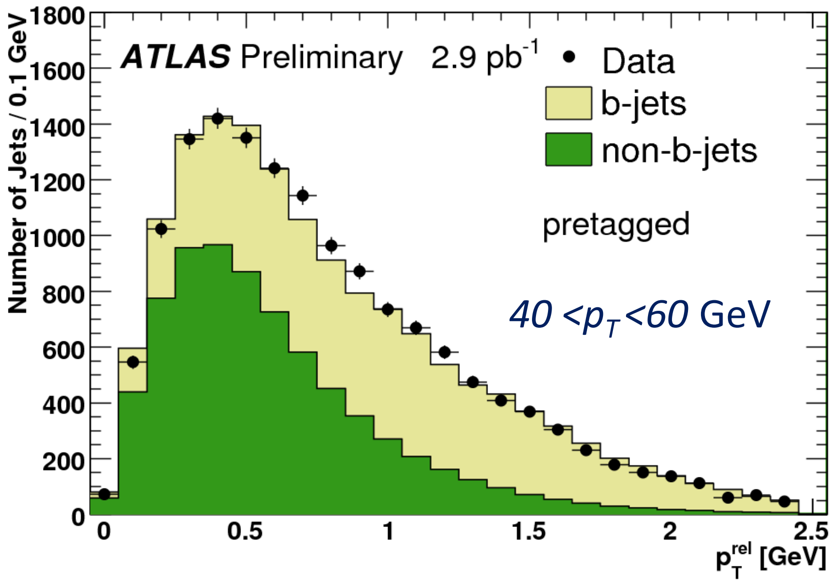

spatial tagging

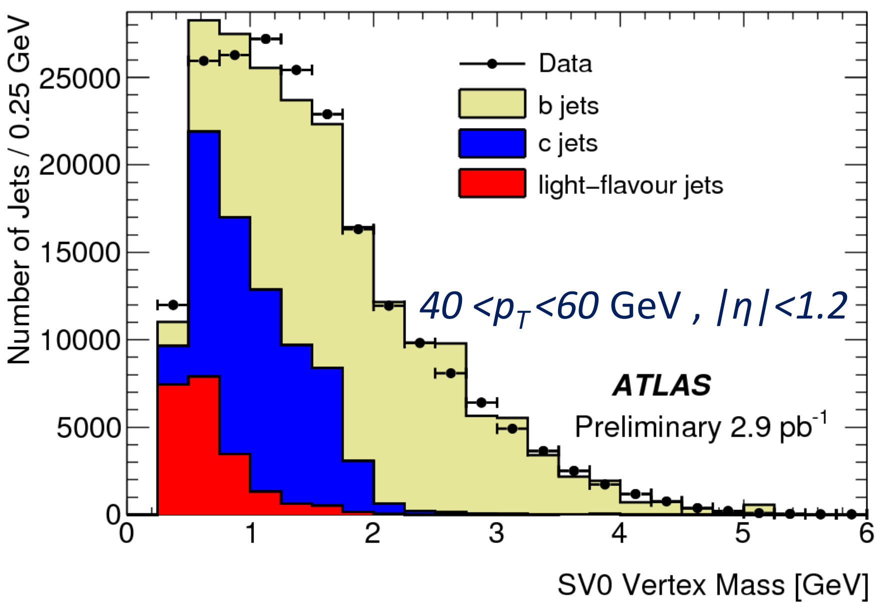

muon+jet (E_T>5 GeV) trigger

anti-k_T (0.4) jets with $25<p_T<85$ GeV, $|\eta|<2.5$

muons with $p_T> 4$ GeV

p_T^{rel} templates taken from simulation (b, c) and data (light-flavour)

variety of jet triggers

jets with $20<p_T<200$ GeV, $|\eta|<2.5$

SV0 mass templates simulated

fractions of b-jets (and c-jets) measured in p_T and $|\eta|$ bins

Summary & Outlook

- $D^{*\pm}$, $D^{\pm}$ and $D_s^{\pm}$ mesons with $p_T > 3.5$ GeV, $|\eta|<2.1$
  $N(D^{*\pm}) = 2020 \pm 120$, $N(D^{\pm}) = 1667 \pm 86$, $N(D_s^{\pm}) = 326 \pm 57$ (stat.)

- $B^{\pm} \to J/\psi\, K^{\pm} \to (\mu^{+}\mu^{-})\, K^{\pm}$ with $p_T > 10$ GeV
  $N(B^{\pm}) = 283 \pm 22$ (stat.)

- $e^{\pm}$ from HQ decays with $E_T > 7$ GeV, $|\eta|<2.0$
  $N(Q \to e) = 9920 \pm 160$ (stat.) $\pm$ 990 (syst.)

- $\mu^{\pm}$ from HQ decays with $p_T > 4$ GeV, $|\eta|<2.5$
  high statistics, prompt $\mu^{\pm}$ fraction measured

- HQ jets with $p_T > 20$ GeV, $|\eta|<2.5$
  high statistics, fractions of b-jets (and c-jets) measured

- Production cross sections soon

- Other methods under study ($D+\mu$, D+jet, double tagged, …)

Back-up Slides

The ATLAS detector

3-level trigger reducing the rate from 40 MHz to ~200 Hz

Length: ~46 m
Radius: ~12 m
Weight: ~7 Ktons

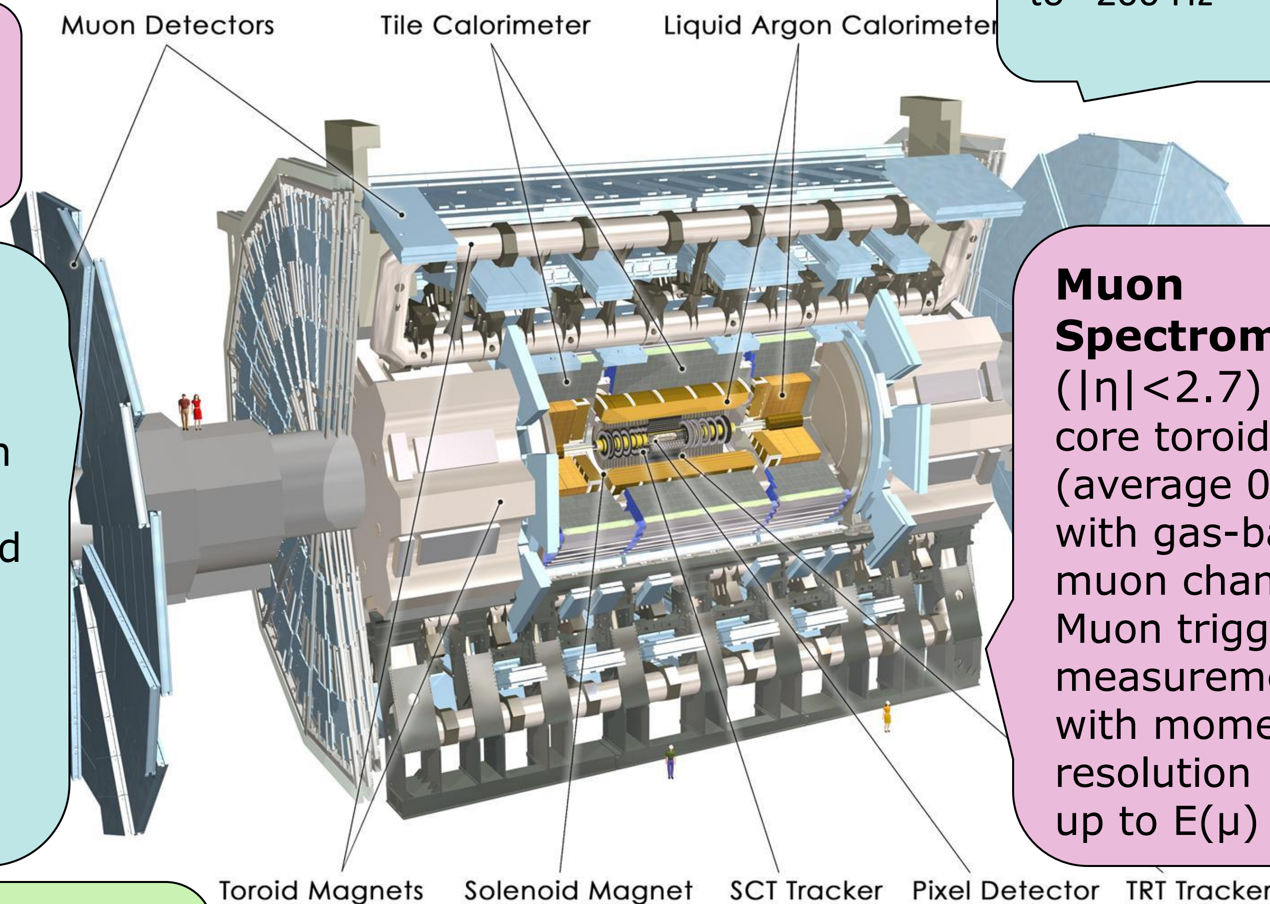

Inner Detector ($|\eta|<2.5$, B=2T): Si Pixels, Si strips, Transition Radiation Tracker (straws). Precise tracking and vertexing, e/π separation. p_t resolution: $\sigma/p_t \sim 3.8\mathrm{x}10^{-4}\ p_t$ (GeV)$\pm$ 0.015

Muon Spectrometer ($|\eta|<2.7$) : air-core toroids (average 0.5T) with gas-based muon chambers. Muon trigger and measurement with momentum resolution < 10% up to E(μ) ~1 TeV

EM calorimeter: Pb-LAr Accordion. e/γ trigger, identification and measurement. E-resolution: $\sigma/E \sim 10\%/\sqrt{E}$

HAD calorimetry ($|\eta|<5$): Fe/scintillator Tiles (central), Cu/W-LAr (fwd). Trigger and measurement of jets and missing ET. E-resolution: $\sigma/E \sim 50\%/\sqrt{E} \pm 0.03$

Tracking with ATLAS Inner Detector

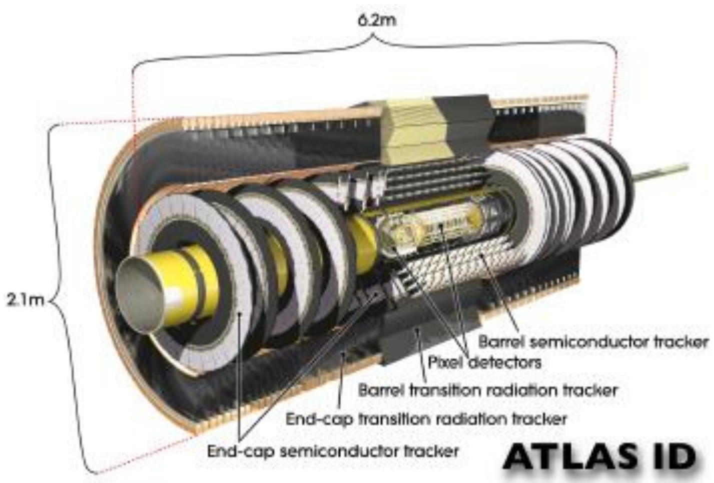

- Pixel Detector:

3 barrel layers, 2 x 3 end-cap discs

$\sigma_{r\phi} \sim 10\ \mu m$, $\sigma_z \sim 115\ \mu m$

- Silicon Strip Detector (SCT)

4 barrel layers, 2 x 9 end-cap discs

$\sigma_{r\phi} \sim 17\ \mu m$, $\sigma_z \sim 580\ \mu m$

- Transition Radiation Tracker(TRT)

73 barrel straw layers, 2x160 end-cap radial straw discs

$\sigma_{r\phi} \sim 130\ \mu m$

Scatter Plot of Hits on Tracks

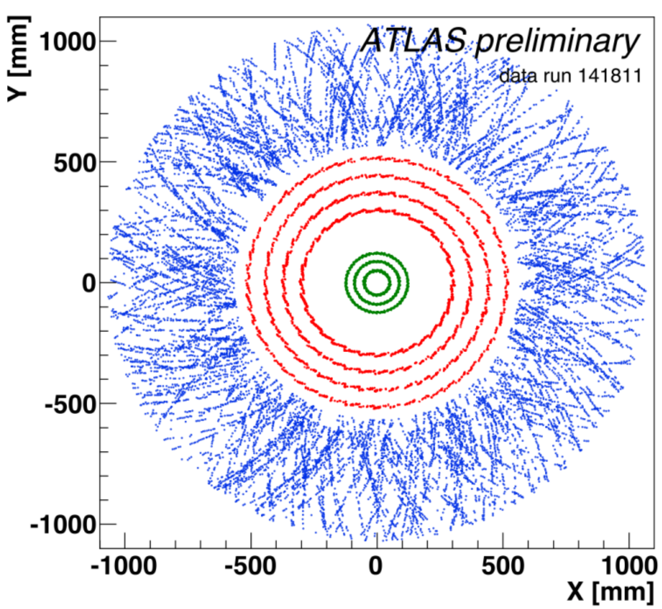

In this analysis:
tracks with at least 1 hit in Pixel and 4 hits in SCT and pT>250 MeV and |η|<2.5

Minimum-Bias Trigger

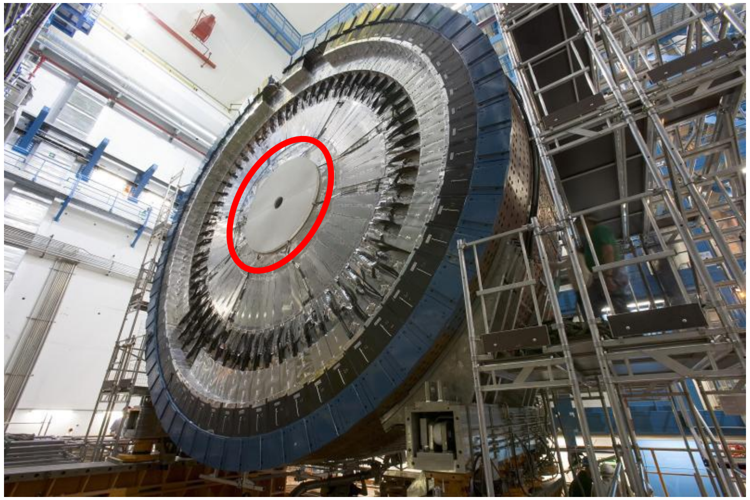

MinBias Trigger Scintillator at z=±3.56 m
on LAr cryostat; 2 rings with 8 sector in azimuth
2.09<|η|<2.82, 2.82<|η|<3.84

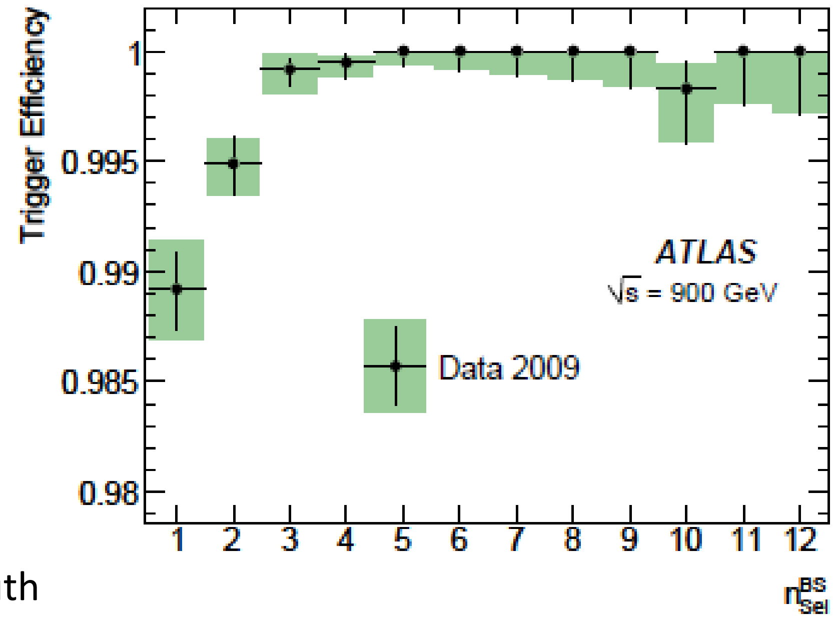

At least one hit above threshold in the Minimum-Bias Trigger Scintillators at each end of the detector

Efficiency is ~100% for events with at least 2 tracks passing beam-spot region

MBTS trigger allow us to measure *D*-mesons production cross-sections without uncertainty originating from trigger efficiency

The trigger is heavily prescaled with luminosity increase

Luminosity and Data Taking

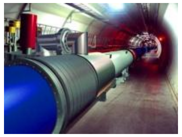

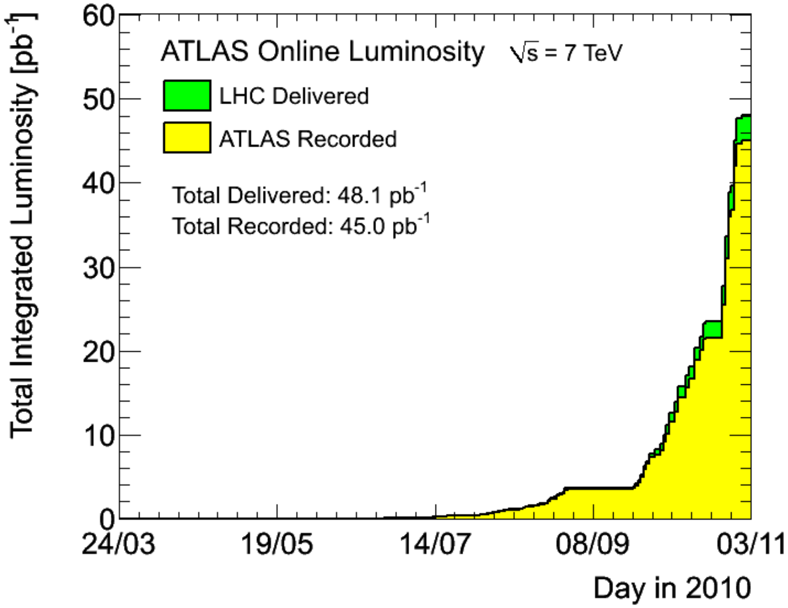

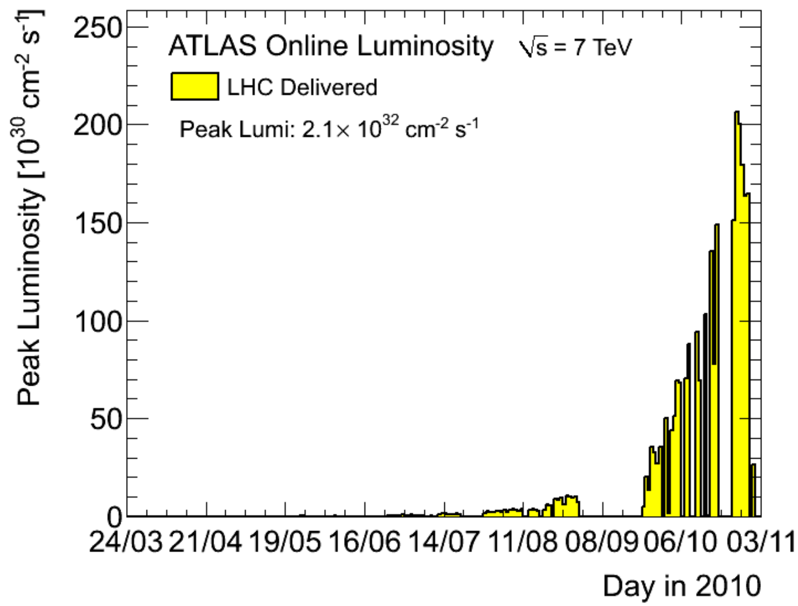

All ID components operational > 97%

Subdetector	Number of Channels	Approximate Operational Fraction
Pixels	80 M	97.5%
SCT Silicon Strips	6.3 M	99.3%
TRT Transition Radiation Tracker	350 k	98.0%

For *D*-meson reconstruction: 1.4 nb^{-1}

(March-May, minimum-bias trigger after prescale)

Resonance reconstruction with secondary and tertiary vertexes

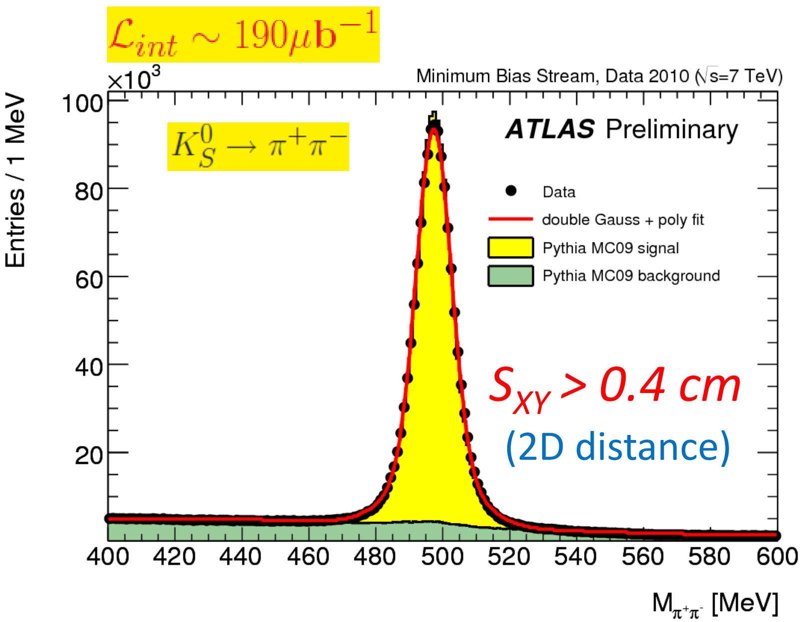

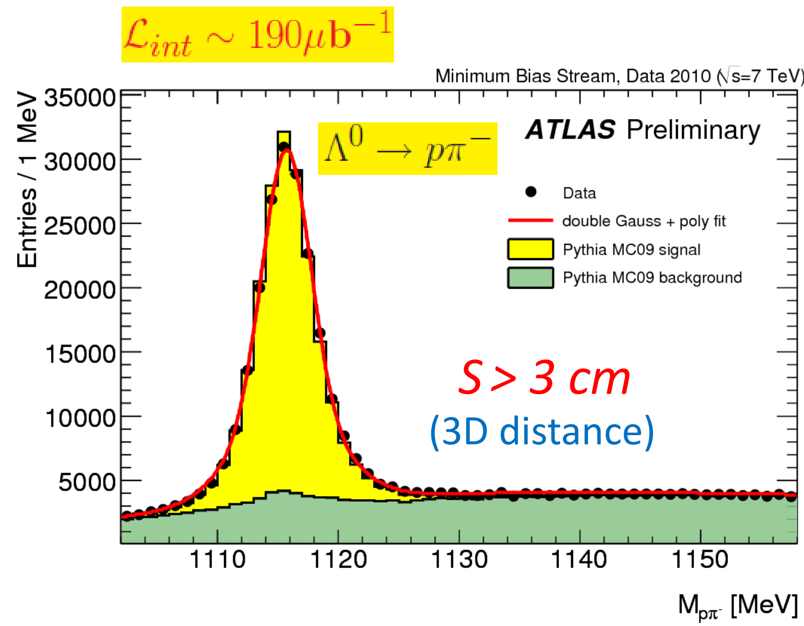

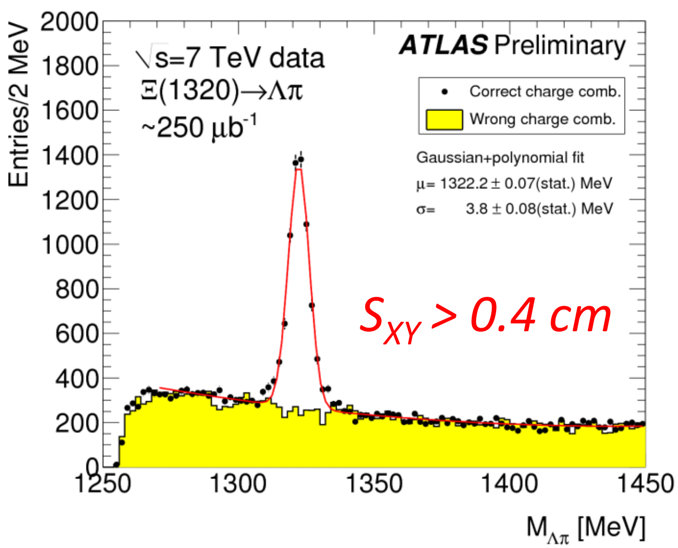

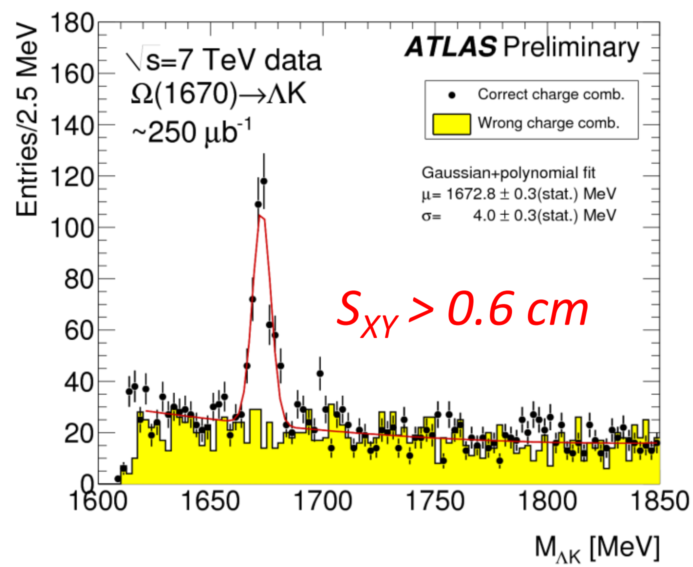

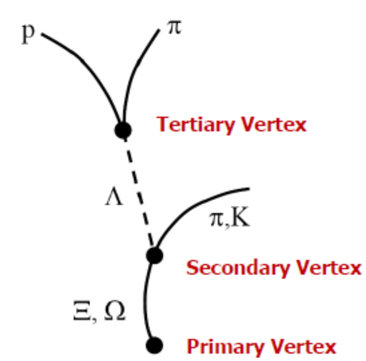

Fitted masses and widths agree with MC and PDG mass values

B^+ and B^- signals